SELF-PROPAGATING COMBUSTION SYNTHESIS OF NANOSTRUCTURED PARTICLES

Andreas Imiolek, Volker Weiser, Stefan Kelzenberg, Evelin Roth, André Lity

Fraunhofer Institut für Chemische Technologie, Joseph-von-Fraunhofer Str. 7, 76327 Pfinztal, Germany

E-Mail: Andreas.Imiolek@ict.fraunhofer.de

ABSTRACT

Apart from the comprehensive investigations of nano-aluminium particle, silicon and boron are also suitable for nano-energetic compositions, but less investigated.

Silicon and boron in combination with different oxidizers yield in efficient composite materials with optimized burning properties. The great reactivity of nanoscale particles is mainly based on their high surface-to-volume-ratio. Porous micrometre-scaled particles with high surface areas should feature similar properties compared to nanoscale particles. Advantages are a much better handling and a distinct lower hazard classification.

In this work, silicon and boron powder with high surface area were synthesized by self-propagating combustion synthesis (SPCS). The characterization of both products (Si, B) was performed using different methods (Raman spectroscopy, XRD, SEM). After washing with hydrochloric acid (10% HCl), the received combustion products showed a high-purity silicon or amorphous boron with a porous sponge-like structure. The particle size ranged between 30 µm – 100 µm.

Keywords: combustion synthesis, amorphous boron, silicon

1 Introduction

The right nanoscale energetic materials mixed with different oxidizers yield in efficient composite materials with optimized burning properties. Up to now, the nano-energetic research has been predominantly focused on the use of aluminium as nano-powder [1]. Silicon and Boron also possess properties, making them suitable candidates for nano-energetic compositions [2, 3]. In general, nanoparticles cause problems during the processing (homogenous dispersion) and the impact on the health and environment is controversial [4]. The great reactivity of nanoscale particles is mainly based on their high surface-to-volume-ratio. Porous micrometre-scale particles of silicon and boron should feature similar properties; advantages are a much better handling and a lower hazard classification.

In this work, we explored synthetic routes to produce nanostructured silicon and boron powder by the magnesium-reduction method. This kind of reaction commonly belongs to the class of "thermite reactions". The term is used to describe a class of exothermic reactions involving a metal reacting with a metallic or non-metallic oxide. The product is a more stable oxide and the corresponding metal or non-metal of the reactant oxide. This form of oxidation-reduction reaction can be written in general form as:

$$M + AO \rightarrow MO + A + \Delta_R H^0 \tag{1}$$

where M is a metal (typically: Mg, Al, Ti, Zr, Zn, etc.), A is ether a metal or a non-metal, MO and AO are their corresponding oxides (B_2O_3, SiO_2, Fe_2O_3, Cr_2O_3, CuO, TiO_2, etc.) and $\Delta_R H^0$ is the standard enthalpy of reaction. As a result of the large exothermic heat, a thermite reaction can generally become self-sustaining, after a local ignition [5, 6].

2   EXPERIMENTAL PROCEDURE

2.1   Combustion Synthesis of the Powders

The materials used in the combustion synthesis of Silicon powder included three different types of SiO$_2$ powder. The main difference is their mean particle size (d) (Quarz I: 0.4 mm – 0.8 mm; Quarz II: < 125 μm and Aerosil: < 50 nm). For the Boron powder synthesis B$_2$O$_3$ powders (90 – 92% purity, particle size 50 – 300 μm) were used as starting material. In all experiments, SiO$_2$ and B$_2$O$_3$ were mixed with Magnesium (99.8% purity, mean particle size d ≤ 44 μm) in stoichiometric ratio (SiO$_2$/Mg = 1/2, (Equation 2); B$_2$O$_3$/Mg = 1/3, (Equation 3)) for several hours by mortar grinder (SiO$_2$) or tumbler mixer (B$_2$O$_3$).

$$2Mg + SiO_2 + \alpha NaCl \rightarrow 2MgO + Si + \alpha NaCl \qquad (2)$$

$$3Mg + B_2O_3 + \alpha NaCl \rightarrow 3MgO + 2B + \alpha NaCl \qquad (3)$$
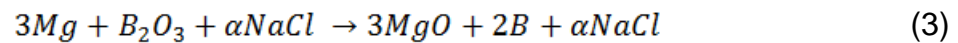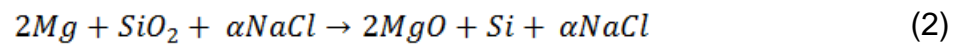
The amount of NaCl added to the main mixture was determined by thermodynamic analysis of the adiabatic temperature (T_{ad}) and will be explained in 3.1.

Samples of about 1 g were filled in a heat-resistant test tube. For ignition, a Bunsen burner (propane) was used.

For the powder characterization, all synthesized samples were washed for 3 h with hydrochloric acid (10% HCl) at 50°C and rinsed with distilled water to eliminate the reaction by-products (MgO, NaCl). Finally the powders were dried in a vacuum oven at 80°C for 48 h.

2.2   Powder Characterization

The characterization of both products (Si, B) was performed using the following methods of analysis. The phase composition of the powders was determined by an X-ray diffraction (XRD) analyser (AXS, Bruker). To study the surface structure of the powders, a field-emission scanning electron microscope (SEM) was used.

The elemental compositions of the powders were examined by the energy-dispersive X-ray spectroscopy (EDX) method. To allow a statement about the purity of the products, Raman spectroscopy (RXN1, Kaiser Opticals) was used.

3 RESULTS AND DISCUSSION

3.1 Thermodynamic Analysis

In a first step, the adiabatic combustion temperatures (T_{ad}) for both reactions, SiO_2 + $2Mg$ + $\alpha NaCl$ and B_2O_3 + $3Mg$ + $\alpha NaCl$, were calculated as a function of the NaCl concentration using EKVI-Code [7]. For the SiO_2 + $2Mg$ + $\alpha NaCl$ system, the results suggested a calculated T_{ad} for a diluent-free mixture ($\alpha=0$) of about 1650°C. This temperature is significantly higher than the melting point of Si (1414°C) and thus prevented the formation of nanostructures. One known method to decrease the adiabatic combustion temperature is to add an inert material to the reactants. NaCl has been recognized as a suitable additive that may lower T_{ad}. As shown in Figure 1 (left), a fast decrease of the adiabatic combustion temperature occurred between 0 mol ≤ α ≤ 0.4 mol. After that, the temperature reaches a plateau (0.4 mol ≤ α ≤ 0.9 mol), followed by a fast decrease with increasing amount of NaCl (1.0 mol ≤ α ≤ 2.8 mol).

Fig. 1 Temperature profile of combustion: SiO_2+$2Mg$+$\alpha NaCl$ system (left) and B_2O_3+$3Mg$+ $\alpha NaCl$ system (right).
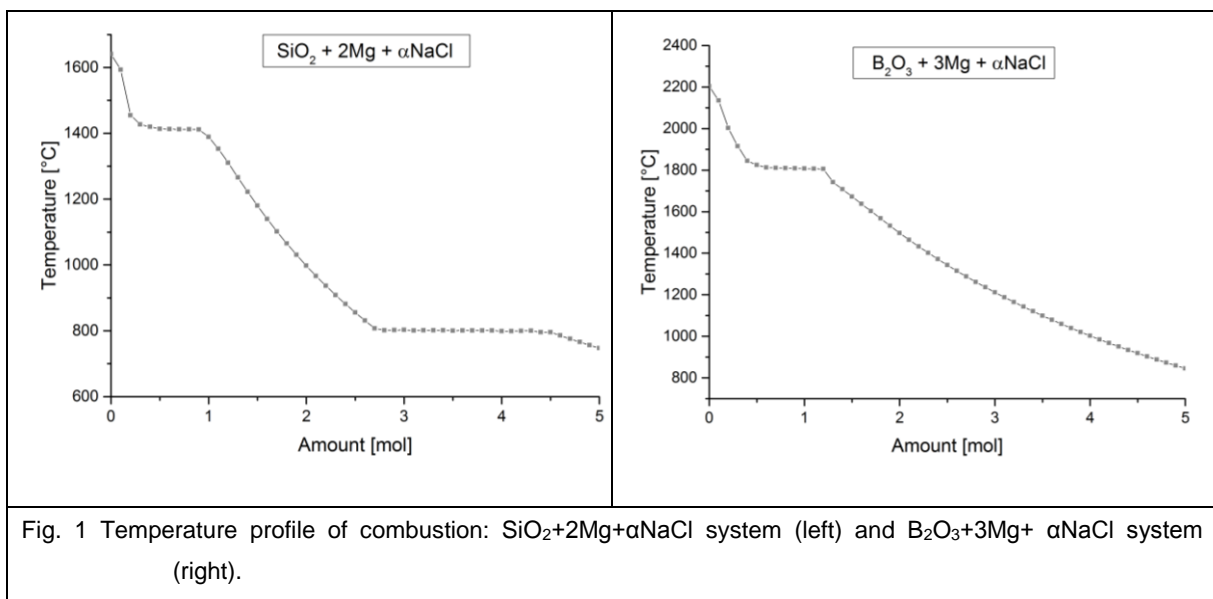
For the $B_2O_3 + 3Mg + \alpha NaCl$ system, the thermodynamic calculations (Figure 1 (right)) predict an adiabatic combustion temperature of 2200°C ($\alpha = 0$), which is also higher than the melting point of boron (2076°C). Already an amount of $\alpha = 0.3$ mol NaCl decreases the temperature to 1915°C. After reaching the plateau between $\alpha = 0.5$ mol and $\alpha = 1.2$ mol, the adiabatic combustion temperature decrease from 1805°C ($\alpha = 1.2$ mol) to 845°C ($\alpha = 5.0$ mol).

For the experimental part, the chosen α – values (Table 1) shall avoid a melting and coarsening of the products (Si, B).

Table 1 Overview of the chosen formation and α – values for the experimental part.

System	Type of SiO_2	α	Predicted T_{ad}
		[mol]	[°C]
$SiO_2 + 2Mg + \alpha NaCl$	Quarz I	2	998
$SiO_2 + 2Mg + \alpha NaCl$	Quarz II	2	998
$SiO_2 + 2Mg + \alpha NaCl$	Aerosil	2	998
$B_2O_3 + 3Mg + \alpha NaCl$		1	1807

3.2 Characterization of the Combustion Products

Typical Raman spectra taken from the base mix, the untreated combustion product and of the purified product for all used SiO_2 types are shown in Figure 2.

The Raman spectra of all initial materials (Quarz I, Quarz II, Aerosil) at $\alpha = 2$ mol displays in total six sharp peaks. Four of them correspond to the sapphire lens of the Raman spectroscope at 418 cm^{-1}, 577 cm^{-1}, 750 cm^{-1} and 1082 cm^{-1} [8]. The predominant signal at 461 cm^{-1} and the one at 355 cm^{-1} are induced by the O-Si-O bending mode of the quartz [9].
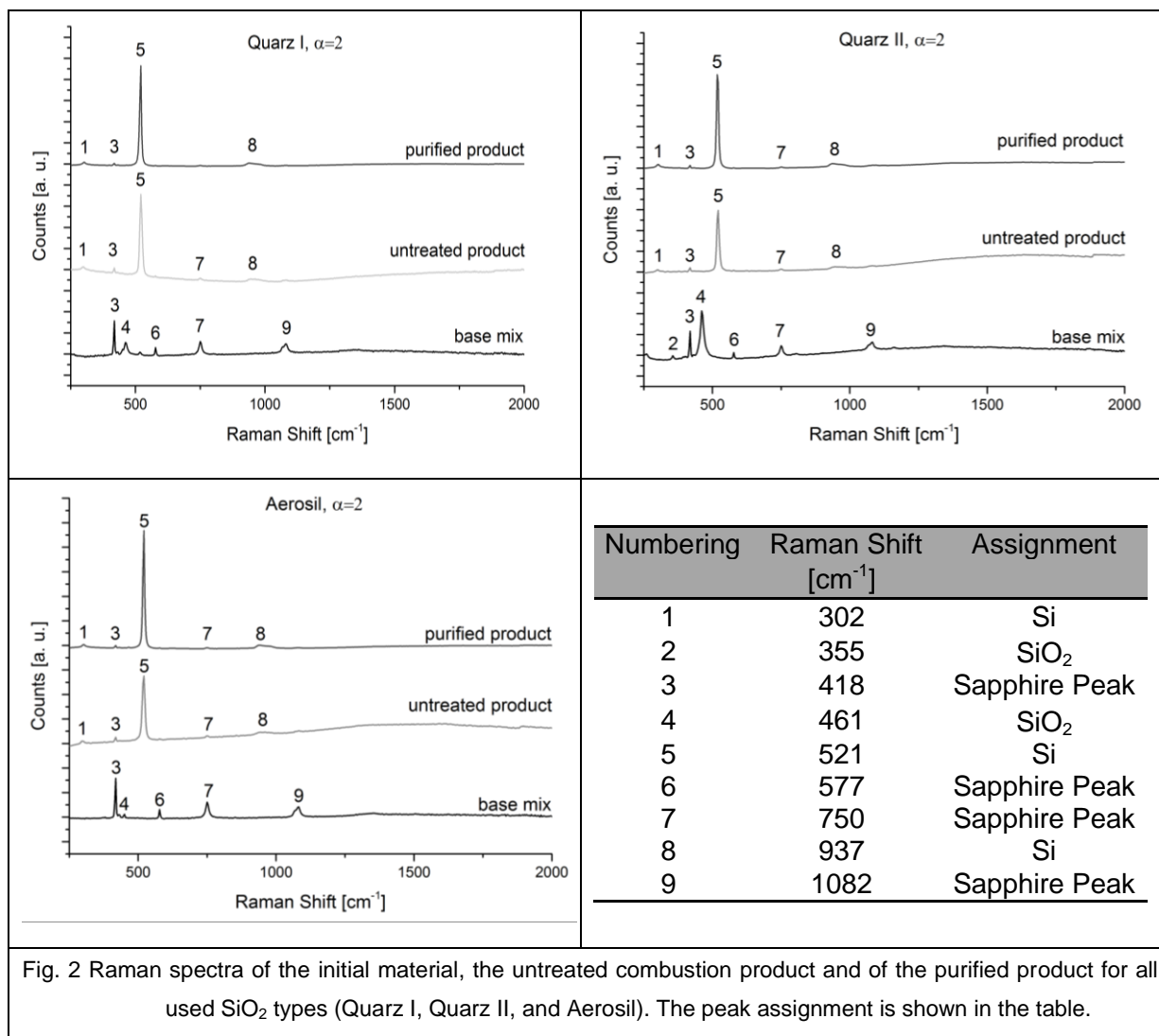
Fig. 2 Raman spectra of the initial material, the untreated combustion product and of the purified product for all used SiO₂ types (Quarz I, Quarz II, and Aerosil). The peak assignment is shown in the table.

| Numbering	Raman Shift [cm⁻¹]	Assignment
1	302	Si
2	355	SiO_2
3	418	Sapphire Peak
4	461	SiO_2
5	521	Si
6	577	Sapphire Peak
7	750	Sapphire Peak
8	937	Si
9	1082	Sapphire Peak

Next, the Raman spectra of the untreated combustion products were compared to those of the base mix. The additional peaks at 302 cm⁻¹, 521 cm⁻¹ and 937 cm⁻¹ are silicon-specific. The latter has the highest intensity and is corresponding to the lattice vibration of crystalline Silicon.

At the first view, the Raman spectra of the purified products have a smooth behaviour compared to the other spectra. The reason is the missing of unreacted Mg and MgO that cause a fluorescent effect.

An analysis of the initial material, untreated product and purified powder of the B_2O_3 + 3Mg + NaCl reaction was renounced. The reason is that the initial material (B_2O_3) and the product (B) are Raman inactive and give no signal.

According to XRD analysis of the $SiO_2 + 2Mg + 2NaCl$ system, the purified combustion products of the three chosen SiO_2 types show typical diffraction peaks of Si, not reacted SiO_2 and the by-product Mg_2SiO_4 (forsterite). The four characteristic silicone signals ($2\Theta = 28.6°$, $47.4°$, $56.2°$ and $76.5°$) were observed in all diffractograms. For the products based on Quarz I and Quarz II as initial materials, the peaks at $2\Theta = 21.0°$, $26.7°$, $36.7°$, $60.1°$ and $68.3°$ are corresponding to the presence of SiO_2. However, the diffractograms of the combustion product with Aerosil as initial material show signals ($2\Theta = 23.0°$, $32.4°$, $35.8°$, $36.6°$, $52.4°$) induced by the by-product (Mg_2SiO_4).
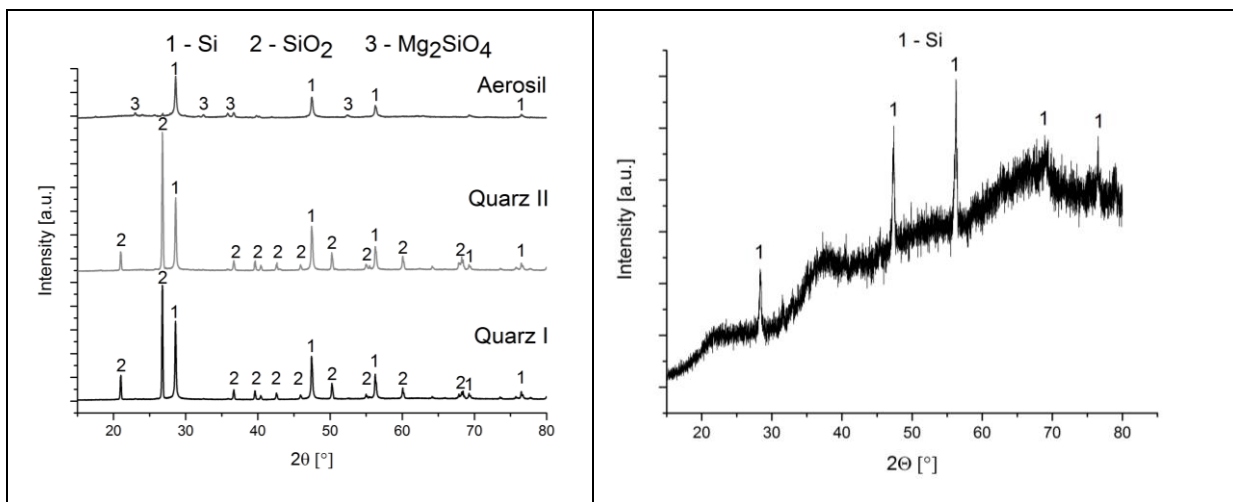
Fig. 3 XRD patterns for the purified combustion products Si (left) and B (right). For the $SiO_2 + 2Mg + 2NaCl$, three different types of SiO_2 were used (Quarz I, Quarz II and Aerosil).

The XRD analysis of the products, based on the $B_2O_3 + 3Mg + NaCl$ thermite reaction, indicate the presence of amorphous boron phase (Figure 3 (right)). The sharp signals at $2\Theta = 28.6°$, $47.1°$ and $56.7°$ are assigned to silicone, which are caused by impurities.

By the application of SEM, the surface of both systems ($SiO_2 + 2Mg + 2NaCl$ and $B_2O_3 + 3Mg + NaCl$) is shown in Figure 4 (a, b). In all cases, regardless of the size and type of the precursors (Quarz I, Quarz II, and Aerosil), the received particles show highly porous sponge-like structures. The particle size of the synthesized material ranges from 30 to 100 µm and is much coarser than corresponding nano-material [10, 11]. The total amount of synthesized products was too less for a BET analysis to determine the total surface area.

Fig. 4 Surface structure and EDX analysis of the products: (a, c) product of SiO_2 + Mg + 2NaCl mixture, (b, d) product of B_2O_3 + Mg + NaCl mixture.
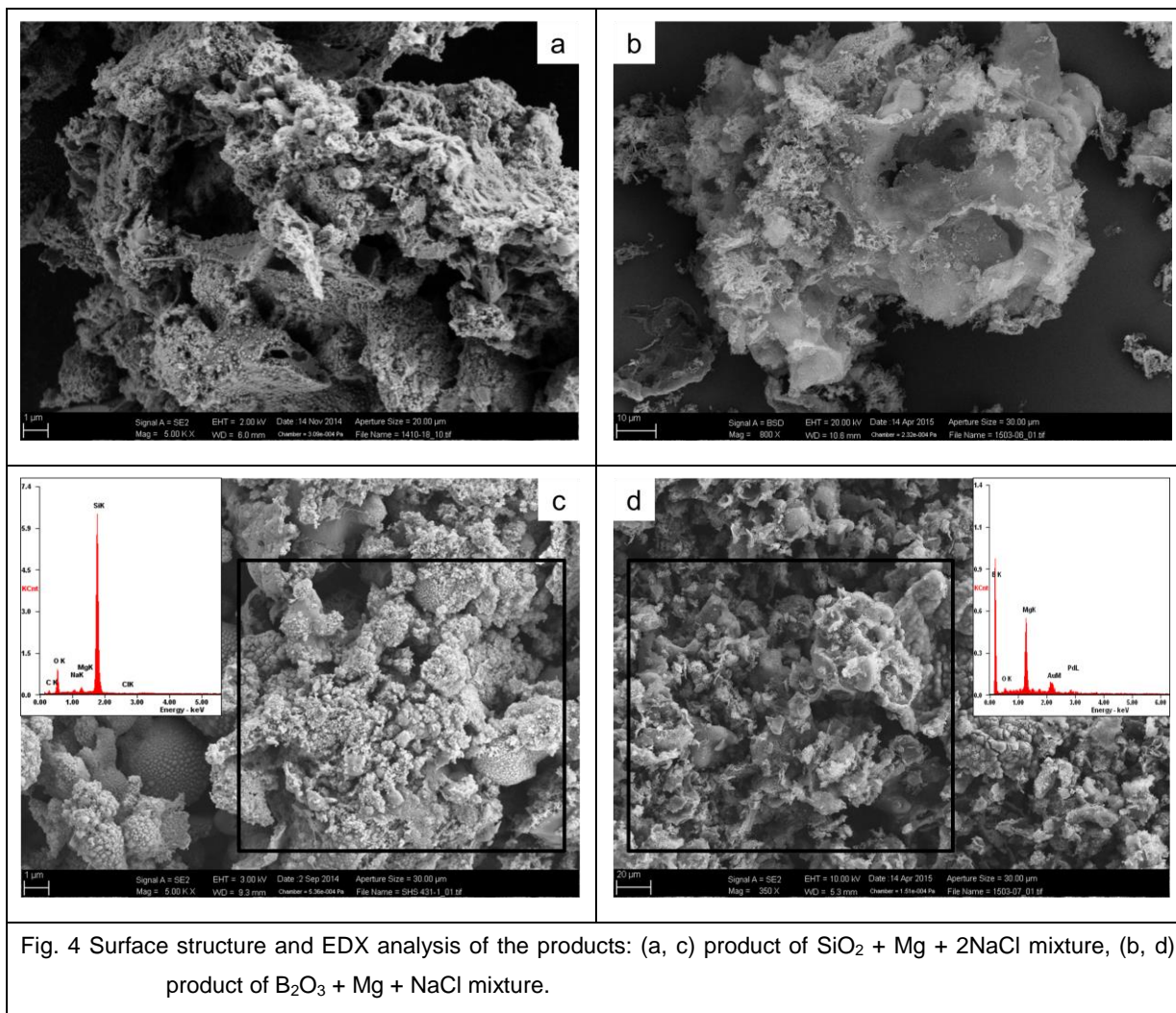
Finally, the qualitative analysis of the elemental composition for both systems was examined using EDX. The powder of the SiO_2 + 2Mg + 2NaCl reaction consists of the elements: Si, Mg, O, Na and Cl (Figure 4c). Therefore, pure silicon is the main product. But SiO_2 may also be present either as passivation layer of Si or unreacted material. Unreacted Mg, MgO, and NaCl as a residue are possible despite the purification.

For the system B_2O_3 + 3Mg + NaCl, the analysed area contained the elements B, Mg and O (Figure 4d). Beside amorphous boron as the main product, by-products like $Mg_3B_2O_6$ are conceivable.

4 CONCLUSION

Self-propagating combustion synthesis (SPCS) was used to produce nanostructured high-surface powders of silicon and boron. For both combustion syntheses, NaCl was added to decrease the combustion temperature of the reaction mixture. On the basis of thermodynamic analysis of the adiabatic temperature (T_{ad}), the added amount of NaCl was determined for the systems. The received products show nanostructured particles in SEM analysis. Raman-spectroscopy, EDX and XRD were used to verify the quality of the synthesized material.

ABBREVIATIONS

SPCS	Self-propagating high-temperature combustion synthesis
Si	Silicon
SiO_2	Silicon Oxide (Quartz)
Mg	Magnesium
MgO	Magnesium Oxide
$MgCl_2$	Magnesium Chloride
Mg_2SiO_4	Forsterite
B	Boron
B_2O_3	Boron Trioxide
NaCl	Sodium chloride
EDX	Energy-Dispersive X-ray spectroscopy
XRD	X-ray diffraction
SEM	Scanning Electron Microscope

REFERENCES

(1) C. D. Yarrington, S. F. Son, T. J. Foley, S. J. Obrey, A. N. Pacheco, Nano Aluminum: The Effect of Synthesis Method on Morphology and Combustion Performance, *Propellants, Explosives, Pyrotechnics*, 2011, 36, 551-557

(2) B. C. Terry, Y. Lin, K. V. Manukyan, A. S. Mukasyan, S. F. Son, L. J. Groven, The Effect if Silicon Powder Chracteristics on the Combustion of Silicon/Teflon/Viton Nanoenergetics, *Propellants Explos. Pyrotech.* **2014**, 39, 337-347.

(3) B. U. Yoo, H. H. Nersisyan, H. Y. Ryu, J. S. Lee, J. H. Lee, Structural and thermal properties of boron nanoparticles synthesized from B2O3 + 3 Mg + k NaCl mixture, Combustion and Flame, **2014**, 161, 3222-3228.

(4) K. L. Dreher, Health and Environmental Impact of Nanotechnology: Toxicological Assessment of Manufactured Nanoparticles, Toxicol Sci., 2004, 77, 3-5

(5) K. V. Manukyan, K. G. Kirakosyan, Y. G. Grigoryan, O. M. Niazyan, A. V. Yeghishyan, A. G. Kirakosyan, S. L. Kharatyan, Mechanism of Molten-Salt-Controlled Thermite Reactions, *Industrial and Engineering Chemistry Research*, **2011**, 50, 10982-10988

(6) L. L. Wang, Z. A. Munir, Y. M. Maximov, Review: Thermite Reactions: Their Utilization in the Synthesis and Processing of Materials, *Journal of Material Science*, **1993**, 3693-3708

(7) B. Noläng, Ekvi System 3.2, *BeN Systems*, Balinge, Sweden, **2004**.

(8) A. Imiolek, Charakterisierung der physikalischen Eigenschaften von PP-CNT Komposite, *Fraunhofer ICT*, **2014**.

(9) T. Ling, A. Wang; Raman Spectroscopy Study of Quartz in Lunar Soils from Apollo 14 and 15 Mission; *National Astronomical Observation*, Beijing; **2012**

(10) Z. Yermekova, Z. Mansurov, A. S. Mukasyan, Combustion Synthesis of Silicon Nanopowders, *International Journal of Self-Propagating High-Temperature Synthesis* **2010**, 19, 2, 94-101.

(11) M. Comet, F. Schnell, V. Pichot, J. Mory, B. Risse, D. Spitzer, Boron as Fuel for Ceramic Thermites, *Energy & Fuels*, **2014**, 28, 4139-4148.